Diabetologia (2012) 55:1167–1178
DOI 10.1007/s00125-011-2427-7

ARTICLE

Deletion of C/EBP homologous protein (*Chop*) in C57Bl/6 mice dissociates obesity from insulin resistance

M. Maris · L. Overbergh · C. Gysemans · A. Waget · A. K. Cardozo · E. Verdrengh · J. P. M. Cunha · T. Gotoh · M. Cnop · D. L. Eizirik · R. Burcelin · C. Mathieu

Received: 16 May 2011 / Accepted: 29 November 2011 / Published online: 12 January 2012

Abstract
Aims/hypothesis Endoplasmic reticulum (ER) stress has been implicated in the development of type 2 diabetes, via effects on obesity, insulin resistance and pancreatic beta cell health. C/EBP homologous protein (CHOP) is induced by ER stress and has a central role in apoptotic execution pathways triggered by ER stress. The aim of this study was to characterise the role of CHOP in obesity and insulin resistance.

Methods Metabolic studies were performed in *Chop*$^{-/-}$ and wild-type C57Bl/6 mice, and included euglycaemic–hyperinsulinaemic clamps and indirect calorimetry. The inflammatory state of liver and adipose tissue was determined by quantitative RT-PCR, immunohistology and macrophage cultures. Viability and absence of ER stress in islets of Langerhans was determined by electron microscopy, islet culture and quantitative RT-PCR.

Results Systemic deletion of *Chop* induced abdominal obesity and hepatic steatosis. Despite marked obesity, *Chop*$^{-/-}$ mice had preserved normal glucose tolerance and insulin sensitivity. This discrepancy was accompanied by lower levels of pro-inflammatory cytokines and less infiltration of immune cells into fat and liver.

Conclusions/interpretation These observations suggest that insulin resistance is not induced by fat accumulation per se, but rather by the inflammation induced by ectopic fat. CHOP may play a key role in the crosstalk between excessive fat deposition and induction of inflammation-mediated insulin resistance.

Keywords CHOP · Endoplasmic reticulum · Inflammation · Obesity · Steatosis · Type 2 diabetes

Abbreviations

ACC	Acetyl-CoA carboxylase
AKT	Thymoma viral proto-oncogene 1
ATF	Activating transcription factor
BMC	Bone mass content
BMD	Bone mass density
C/EBP	CCAAT enhancer binding protein
CHOP	C/EBP homologous protein
ChREBP	Carbohydrate responsive element binding protein
ER	Endoplasmic reticulum

Electronic supplementary material The online version of this article (doi:10.1007/s00125-011-2427-7) contains peer-reviewed but unedited supplementary material, which is available to authorised users.

M. Maris · L. Overbergh (✉) · C. Gysemans · E. Verdrengh · J. P. M. Cunha · C. Mathieu
Laboratory for Experimental Medicine and Endocrinology (LEGENDO), Catholic University of Leuven,
Herestraat 49 bus 902,
3000 Leuven, Belgium
e-mail: lutgart.overbergh@med.kuleuven.be

A. Waget · R. Burcelin
Institute of Molecular Medicine, Rangueil Hospital,
Toulouse, France

A. K. Cardozo · M. Cnop · D. L. Eizirik
Laboratory of Experimental Medicine,
Université Libre de Bruxelles (ULB),
Brussels, Belgium

T. Gotoh
Department of School Health,
Faculty of Education & Department of Molecular Genetics,
Kumamoto University,
Kumamoto, Japan

M. Cnop
Division of Endocrinology, Erasmus Hospital,
Université Libre de Bruxelles (ULB),
Brussels, Belgium

ERO1α	ER oxidase 1α
FAS	Fatty acid synthase
GRP78	Glucose-regulated protein 78
HK2	Hexokinase 2
LPS	Lipopolysaccharide
MCP1	Monocyte chemotactic protein 1
ROS	Reactive oxygen species
SOCS3	Suppressor of cytokine signalling 3
SREBP	Sterol regulatory element binding protein
WT	Wild type
XBP-1s	X-box binding protein 1 spliced

Introduction

Growing evidence shows that endoplasmic reticulum (ER) stress is an important mechanism linking obesity, insulin resistance and glucose intolerance [1, 2]. Several reports have demonstrated that ER stress markers are upregulated in the liver and fat of obese mouse models [2] and that ER stress in the hypothalamus is associated with central insulin and leptin resistance, hyperphagia and weight gain [3].

C/EBP homologous protein (CHOP) is a 29 kDa protein regulating ER-stress-mediated apoptosis [4]. Downstream of *Chop*, different apoptotic effectors have been reported [5], but overall, *Chop*-induced signalling is not well understood. Overexpression of *Chop* decreases B cell CLL/lymphoma 2 (BCL-2) protein levels and causes translocation of BCL2-associated X protein (BAX) protein from the cytosol to the mitochondria, transmitting the death signal to the mitochondria [6]. Progressive hyperglycaemia in the Akita mouse, a model spontaneously developing hyperglycaemia with reduced beta cell mass [7], is accompanied by *Chop* induction and beta cell apoptosis, but deletion of *Chop* delayed onset of diabetes in heterozygous Akita mice [8]. CHOP is also involved in the development of obesity [9] and regulation of inflammation [10–13]. Lung damage induced by lipopolysaccharide (LPS) treatment is attenuated in $Chop^{-/-}$ mice, suggesting that the ER-stress pathway involving CHOP is activated and displays a role in the pathogenesis of septic shock lung. Attenuation of IL-1β activity in broncho-alveolar lavage fluid of $Chop^{-/-}$ mice and suppression of caspase-11, which is needed for the activation of procaspase-1 and pro-IL-1β, have been demonstrated [10, 11]. It has been suggested that LPS, a Toll-like receptor 4 (TLR4) ligand, induces a marked increase in protein synthesis, leading to prolonged ER stress during LPS–TLR4 signalling [14]. In addition, LPS caused accelerated upregulation of ER-stress-response genes such as *Chop* and pro-inflammatory cytokine genes [15], but the underlying molecular mechanisms of LPS-induced ER stress are not well understood. $Chop^{-/-}$ mice also show low expression levels of caspase-1 and -11 and *Il-1β* (also known as *Il1b*) in chemically induced pancreatitis, whereas these mediators are strongly upregulated when pancreatitis is induced in control mice. As a result, *Chop* deletion results in suppressed apoptosis of acinar cells and lower infiltration of inflammatory cells in the pancreas [13]. A role for *Chop* was also described in experimental colitis: when colitis was induced, the elevation of mRNA expression levels of *Mac-1* (also known as *Itgam*), *Ero1α* (also known as *Ero1l*) and caspase-11 was suppressed in $Chop^{-/-}$ compared with wild-type mice. As a result, it was suggested that CHOP activity involves various

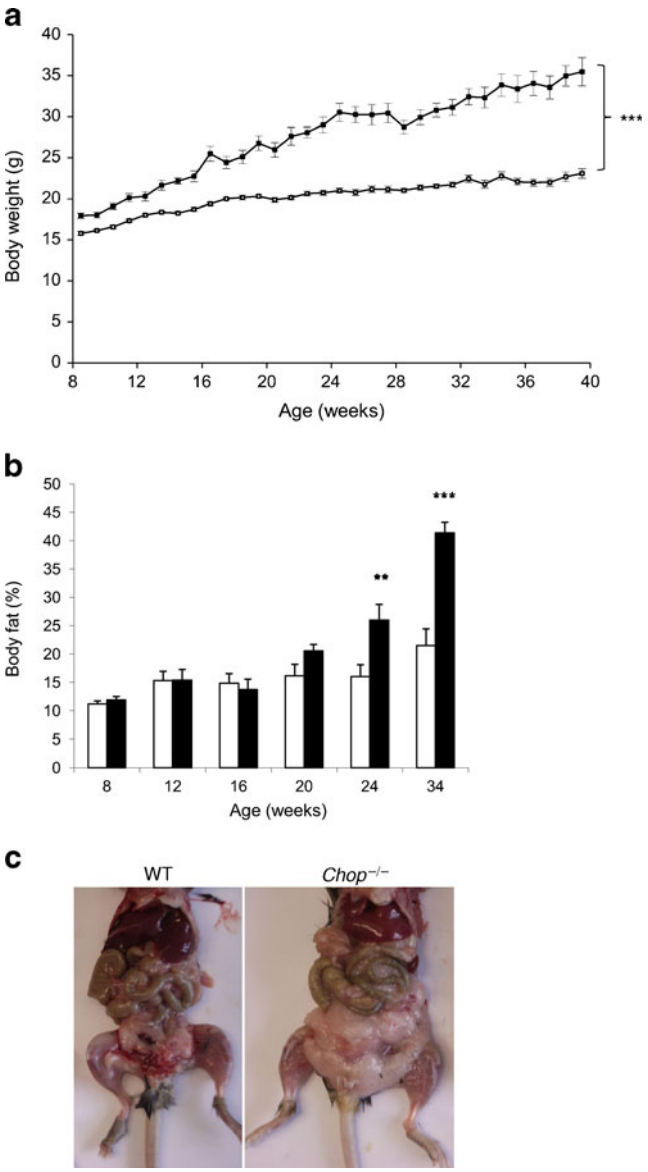

Fig. 1 Body weight and body fat percentage of female WT and $Chop^{-/-}$ mice. Body weight (**a**), percentage of body fat (**b**) of female WT (white bars) and $Chop^{-/-}$ (black bars) mice and representative WT and $Chop^{-/-}$ mice photographed at 24 weeks of age (**c**). Body weight was measured weekly, whereas body fat was measured at 8, 12, 16, 24 and 34 weeks of age using dual X-ray absorptiometry. Data are shown as the means±SEM (n=8). $^{**}p<0.01$ and $^{***}p<0.001$ vs WT mice

stimulatory mechanisms, such as macrophage infiltration via induction of macrophage-1 antigen (MAC-1), reactive oxygen species (ROS) production via ER oxidase 1α (ERO1α) and IL-1β production via caspase-11, all resulting in mucosal cell apoptosis [12]. Finally, it has been demonstrated that CHOP is an inhibitor of the wingless-Int (WNT) signalling pathway and is necessary for normal bone development as *Chop* overexpression induced osteopenia [16].

The aim of the present study was to define the in vivo role of CHOP in obesity and insulin resistance by studying the effects of systemic deletion of this transcription factor in mice.

Methods

Details of the islets and peritoneal macrophage isolation and culture, transmission electron microscopy quantitative RT-PCR and western blot analysis are available in the electronic supplementary material (ESM).

Animals Female C57Bl/6 (wild type [WT]) (Harlan, Horst, the Netherlands) and *Chop*$^{-/-}$ mice (provided by S. Akira [Osaka University, Japan] and M. Mori [Kumamoto University, Japan]) [17], backcrossed ten generations on a C57Bl/6 background, were maintained on regular chow containing 70% energy from carbohydrate, 20% from protein and 10% from fat (Research Diets #D12450B; Research Diets, New Brunswick, NJ, USA), and housed on a 12 h light/dark cycle. For experiments in the fasted state, mice were fasted overnight and kept in a separate cage for the indicated period of time. All animal experimental procedures were approved by the Ethics Commission of KULeuven.

Whole body dual-energy X-ray absorptiometry Fat percentage, bone mass content (BMC) and bone mass density (BMD) were measured in vivo by dual-energy X-ray absorptiometry (DEXA; PIXImus densitometer; Lunar, Madison, WI, USA), using an ultra-high resolution (0.18×0.18 pixels, resolution of 1.6 line pairs/mm) and software version 1.45.

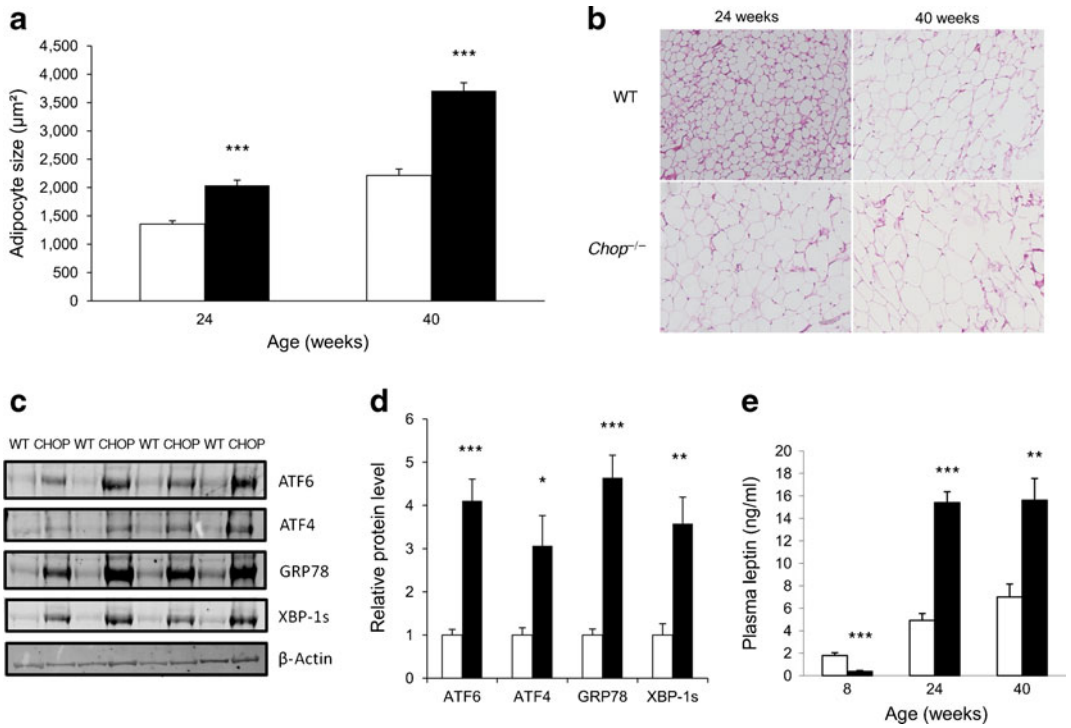

Fig. 2 Adipocyte size, ER-stress markers and leptin levels in WT and *Chop*$^{-/-}$ mice. **a** Adipocyte size of WT (white bars) and *Chop*$^{-/-}$ (black bars) mice at 24 and 40 weeks of age. Adipocyte cell size was measured by determining the diameter of at least 50 cells in four different microscopic fields in fat pads of two different mice (×20 magnification). $^{***}p<0.001$ vs WT mice. **b** H&E staining of representative adipocyte sections of 24- and 40-week-old mice of the genotypes indicated. Photomicrographs (×20 magnification) were captured with a Zeiss Axiovert microscope and analysed with Axiovison Rel. 4.6 software. The pictures are representative of observations made in two different mice. **c** Western blotting for the ER-stress markers ATF6, ATF4, GRP78, XBP-1 s and stable housekeeping protein β-actin on total abdominal fat extracts of female WT and *Chop*$^{-/-}$ mice at 24 weeks of age (n=4). **d** Relative protein level normalised to the stable housekeeping protein β-actin in total abdominal fat extracts of female WT (white bars) and *Chop*$^{-/-}$ mice (black bars) at 24 weeks of age. Results are means±SEM (n=4 independent experiments). $^{*}p<0.05$; $^{**}p<0.01$; $^{***}p<0.001$ vs WT mice. **e** Plasma leptin levels of WT (white bars) and *Chop*$^{-/-}$ mice (black bars) at 8, 24 and 40 weeks of age. Data are shown as the means±SEM (n=8). $^{**}p<0.01$ and $^{***}p<0.001$ vs WT mice

Histology and immunohistochemistry Abdominal adipose tissue, liver, skeletal muscle and pancreas were fixed in 10% (vol./vol.) formaldehyde and embedded in paraffin. Tissues were sectioned in 5 μm slices and stained with haematoxylin and eosin. Photomicrographs were captured with a Zeiss Axiovert microscope (Carl Zeiss, Oberkochen, Germany) and analysed with Axiovision Rel.4.6 software. Adipocyte cell size was measured by determining the size of at least 50 adipocytes in four microscopic fields in fat pads from each mouse (×20 magnification). Islet size was measured by acquiring images from eight to ten distal, random, non-overlapping images of haematoxylin and eosin-stained pancreatic sections (×10 magnification).

Oil red O was used to stain neutral lipids in frozen sections of muscle, liver and pancreas. For immunohistochemistry, paraffin sections were stained for T cells using rabbit anti-CD3 (Dako, Glostrup, Denmark) and for macrophages using rat anti-F4/80 (Serotec, Düsseldorf, Germany).

Metabolic studies Blood glucose levels were determined from tail vein blood samples using an Accu-Chek Aviva glucose meter (Roche Diagnostics, Vilvoorde, Belgium).

For the glucose tolerance test, mice were fasted overnight and injected intraperitoneally with glucose solution (2 g/kg). Blood glucose concentrations were determined before and at 15, 30, 60, 90 and 120 min after injection. Insulin, leptin and adiponectin levels were measured in plasma by ELISA using insulin standards (Mercodia, Uppsala, Sweden), leptin standards (Crystal Chem, Chicago, IL, USA) and adiponectin standards (Millipore, Billerica, MA, USA), respectively.

Plasma triacylglycerol levels were determined by means of a coupled enzymatic assay previously described [18] but adapted to 96-well plate readers and omitting the lipid extraction step (final volume 250 μl). Analysis of plasma NEFA was done by a coupled enzymatic assay [19], using a commercial kit (NEFA C kit; Wako, Neuss, Germany) adapted to 96-well plates (final volume 240 μl).

Plasma levels of alanine aminotransferase, aspartate aminotransferase and alkaline phosphatase were determined by enzymatic assays using commercial kits (Roche/Hitachi Modular Analytics, Laval, Canada).

Plasma levels of T_3 and T_4 were measured by radioimmunoassay as described previously [20].

Euglycaemic–hyperinsulinaemic clamp studies Euglycaemic–hyperinsulinaemic clamp studies were performed on 24-week-old female *Chop*$^{-/-}$ and WT mice as previously described [21]. Insulin was infused at a rate of 18 mU kg^{-1} min^{-1} for 3 h, whereas euglycaemia was maintained by periodically adjusting the 15% (wt/vol.) glucose infusion rate. Glucose turnover and hepatic glucose production rates were calculated as previously described [21].

For measuring specifically insulin signalling in liver and skeletal muscle, overnight-fasted (16 h) 24-week-old female *Chop*$^{-/-}$ and WT mice were anaesthetised by intraperitoneal injection of avertin (0.02 ml/g body weight; Fluka Chemica, Bornem, Belgium). Human insulin, 5 U, (Actrapid; Novo Nordisk, Bagsvaerd, Denmark) or NaCl solution was injected through the vena cava inferior. After 5 min, liver, abdominal fat tissue and hindlimb muscles were removed and lysates were subjected to western blotting [22].

Indirect calorimetric and ambulatory activity At 24 weeks of age, the energy expenditure of WT and female *Chop*$^{-/-}$ mice was measured for 24 h by indirect calorimetry (Oxylet; Panlab-Bioseb, Chaville, France). Mice were scored for oxygen consumption ($\dot{V}O_2$), carbon dioxide production ($\dot{V}CO_2$), ambulatory activity and energy expenditure (calculated according to the following formula:

$$1.44 \times \dot{V}O_2 \times (3.815 + 1.232 \times RQ)$$

$\dot{V}O_2$ and $\dot{V}CO_2$ were measured over a 24 h period. Ambulatory activities of the mice were monitored by an infrared photocell-beam-interruption method (Sedacom; Panlab-Bioseb).

Statistical analysis For all experiments, comparisons were performed by a two-sided unpaired *t* test. $p<0.05$ was considered statistically significant. The data are presented as means±SEM.

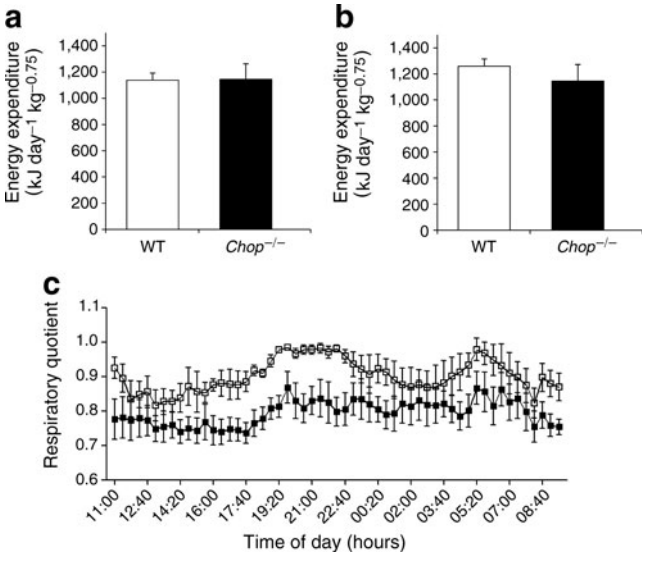

Fig. 3 Energy expenditure and RQ of WT and *Chop*$^{-/-}$ mice at 24 weeks of age. Energy expenditure, expressed as kJ day^{-1} metabolic weight^{-1}, of WT (white bars) and *Chop*$^{-/-}$ mice (black bars) at 24 weeks of age during daylight (**a**) and night time (**b**). Data are shown as the means±SEM (n=4). **c** Recording over 24 h of RQ of WT (white squares) and *Chop*$^{-/-}$ mice (black squares) at 24 weeks of age. Data are shown as the means±SEM (n=4)

Results

Chop deletion induces obesity At 8 weeks of age, body weight was higher in *Chop*$^{-/-}$ mice and they gained progressively more weight compared with WT mice (Fig. 1a). Body composition revealed no difference in percentage body fat up to 16 weeks of age. At 20 weeks of age, body fat tended to increase in *Chop*$^{-/-}$ compared with WT mice (20.5%±1.2 vs 16.2%±2.0; p=0.08) and it was significantly higher from week 24 onwards (Fig. 1b). *Chop*$^{-/-}$ mice showed mainly an increase in abdominal fat (Fig. 1c). The adipocyte size in abdominal fat pads of *Chop*$^{-/-}$ mice was 34% and 41% larger compared with WT mice at 24 and 40 weeks of age, respectively (Fig. 2a,b). Compared with WT mice, the hypertrophic adipocytes of *Chop*$^{-/-}$ mice showed increased protein levels of the typical ER-stress markers glucose-regulated protein 78 (GRP78), X-box binding protein 1 spliced (XBP-1s) and activating transcription factor (ATF) 4 and 6 (Fig. 2c,d), whereas no differences could be observed in mRNA expression levels of these markers in *Chop*$^{-/-}$ compared with WT mice (ESM Fig. 1a).

Levels of mRNA expression of *C/ebpα* (also known as *Cebpa*) (2.0±0.5 vs 1.7±0.5; NS) and *Pparγ* (also known as *Pparg*) (1.2±0.1 vs 1.2±0.1; NS) in abdominal fat tissue were comparable between *Chop*$^{-/-}$ and WT mice, whereas *C/ebpβ* (also known as *Cebpb*) expression was lower in *Chop*$^{-/-}$ mice compared with WT mice (0.2±0.03 vs 0.3±0.03; p<0.05). Expression levels of mRNA encoding carbohydrate responsive element binding protein (ChREBP) and sterol regulatory element binding protein (SREBP), as well as of hexokinase 2 (HK2), acetyl-CoA carboxylase (ACC) and fatty acid synthase (FAS) were not different in the abdominal fat tissue of *Chop*$^{-/-}$ and WT mice (ESM Fig. 1c).

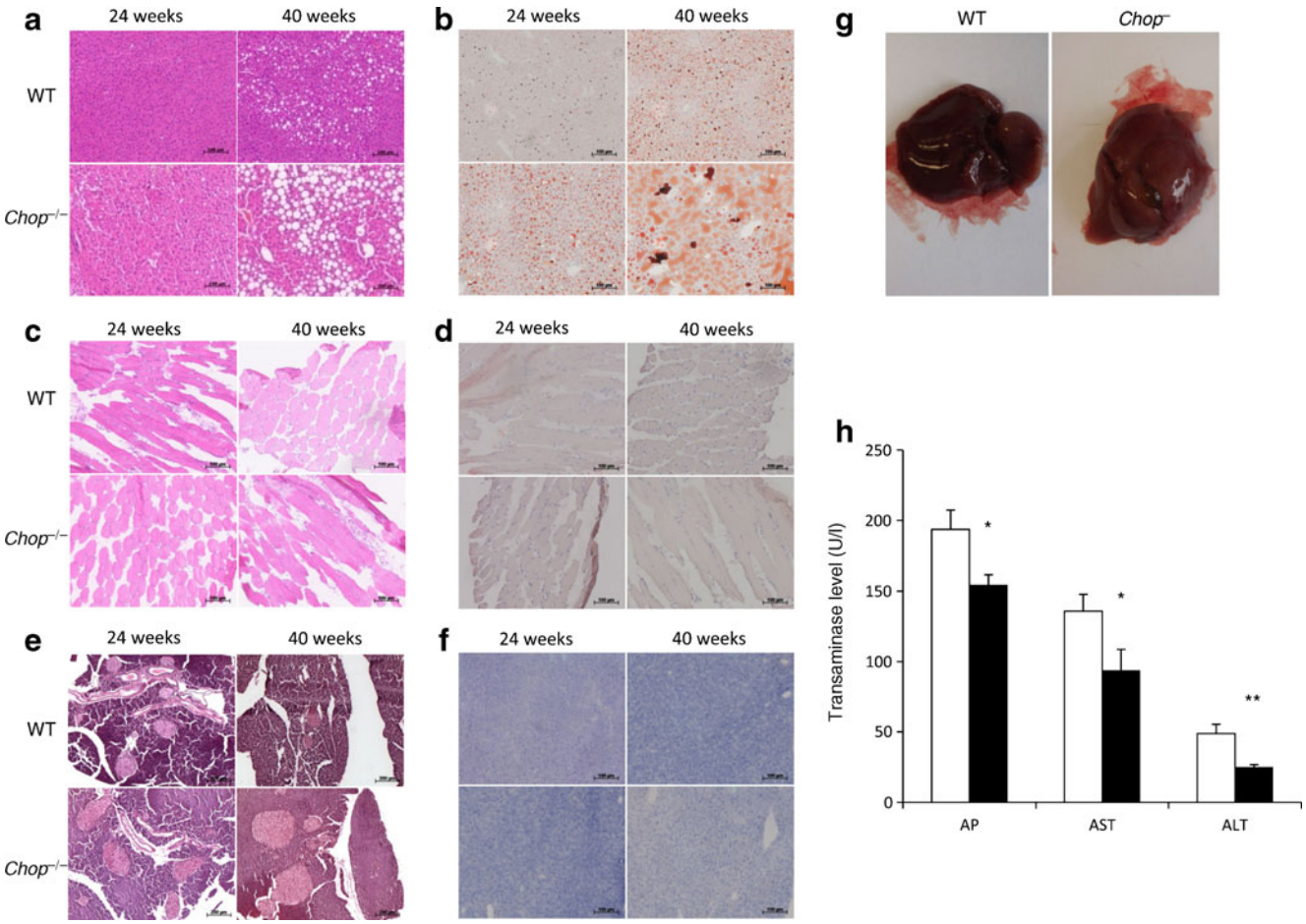

Fig. 4 **a–f** H&E and Oil Red O staining of liver, muscle and pancreas and liver enzymes of WT and *Chop*$^{-/-}$ mice. H&E (**a,c,e**) and Oil Red O (**b,d,f**) staining of representative (of two independent observations) liver (**a,b**), skeletal muscle (**c,d**) and pancreas (**e,f**) sections from mice of the indicated genotypes at 24 and 40 weeks of age. Photomicrographs were captured with a Zeiss Axiovert microscope and analysed with the Axiovison Rel. 4.6 software. **g** Representative liver of female WT and *Chop*$^{-/-}$ mice photographed at 24 weeks of age. **h** Levels of the transaminases alkaline phosphatase, aspartate aminotransferase and alanine aminotransferase in WT (white bars) and *Chop*$^{-/-}$ mice (black bars) at 24 weeks of age. Data are shown as the means±SEM (n=6). $^{*}p$<0.05 and $^{**}p$<0.01 vs WT mice. ALT, alanine aminotransferase; AP, alkaline phosphatase; AST, aspartate aminotransferase

The increase in fat mass in *Chop*$^{-/-}$ mice was accompanied by an increase in BMC and BMD (ESM Fig. 2a,b), as well as by increased plasma leptin levels (Fig. 2e). *Chop*$^{-/-}$ mice showed a trend to higher cumulative food intake compared with WT mice (3.56±0.74 vs 1.91±0.39 g/day; p=0.09). Energy expenditure was similar in *Chop*$^{-/-}$ and WT mice, both during daylight and night time (Fig. 3a,b), whereas the RQ of *Chop*$^{-/-}$ mice was lower compared with WT mice (Fig. 3c). Plasma levels of thyroid hormones T3 and T4, mRNA expression levels of *Ucp1* in brown adipose tissue and cage movements were similar between *Chop*$^{-/-}$ and WT mice (ESM Fig. 3).

Chop deletion induces hepatic fat accumulation At 24 weeks of age, *Chop*$^{-/-}$ mice showed increased fat deposition in liver compared with WT mice (Fig. 4a,b,g), whereas no difference in fat deposition could be detected in skeletal muscle (Fig. 4c,d) and pancreas (Fig. 4e,f). Liver enzyme levels were lower in *Chop*$^{-/-}$ mice (Fig. 4h) and mRNA (ESM Fig. 1b) as well as protein levels of the major ER-stress markers GRP78 and XBP-1s were not altered in *Chop*$^{-/-}$ compared with WT mice (ESM Fig. 4a,b).

No differences were detected in plasma NEFA and triacylglycerol levels between WT and *Chop*$^{-/-}$ mice at 24 and 40 weeks of age (ESM Fig. 4c,d).

Levels of mRNA expression of *Chrebp* (also known as *Mlxipl*), *Srebp* (also known as *Srebf1*), *Hk2*, *Acc* (also known as *Acaca*) and *Fas* (also known as *Fasn*) were not different in the livers of *Chop*$^{-/-}$ and WT mice (ESM Fig. 5a). In addition, nuclear protein levels of ChREBP and SREBP, as well as total ACC and FAS protein levels were unchanged in liver of *Chop*$^{-/-}$ compared with WT mice at 24 weeks of age (ESM Fig. 5b).

Chop$^{-/-}$ *mice maintain a normal glycaemia, but Chop deletion does not protect islets* *Chop*$^{-/-}$ mice showed normal fasting glycaemia (2.82±0.27 vs 3.13±0.27 mmol/l in WT mice; NS) and glucose tolerance remained comparable between *Chop*$^{-/-}$ and WT mice (ESM Fig. 6). Plasma insulin levels were higher in *Chop*$^{-/-}$ mice at 24 weeks of age (149.18±16.53 vs 99.35±3.83 pmol/l in WT mice; p<0.05), which was associated with increased total islet size (17,256±1443 vs 8,954±719 μm^2 in WT mice; p<0.001). Electron microscopy of beta cells did not reveal any changes in ER structure between *Chop*$^{-/-}$ and WT islets (ESM Fig. 7a). No signs of apoptosis were observed in islets of *Chop*$^{-/-}$ and WT mice after exposure to thapsigargin for 48 h (92.4%±1.4 and 93.3%±2.3% of living islet cells in *Chop*$^{-/-}$ and WT mice, respectively, vs 95.6%±1.1 and 96.4%±0.2 of living islet cells in control conditions in *Chop*$^{-/-}$ and WT mice, respectively). Exposure of islets to unsaturated or saturated NEFA, thapsigargin or the combination of IL-1 and IFN-γ for 5 days caused similar apoptotic rates in *Chop*$^{-/-}$ and WT islets (ESM Fig. 7b).

Chop$^{-/-}$ *mice maintain normal insulin sensitivity* The glucose turnover rate, glycolysis and glycogen synthesis rates, as measured by euglycaemic–hyperinsulinaemic clamps at 24 weeks of age, were similar in WT and *Chop*$^{-/-}$ mice (Fig. 5a–c). Hepatic glucose production (−5.87±3.81 vs −4.79±4.83 mg kg^{-1} min^{-1} in *Chop*$^{-/-}$ and WT mice, respectively; NS), as well as the level of serine and threonine phosphorylated thymoma viral proto-oncogene 1 (AKT) levels, were similar in liver of *Chop*$^{-/-}$ and WT mice (Fig. 5d,e), all confirming sustained hepatic insulin signalling. Hepatic insulin signalling was further corroborated as p(Ser)AKT phosphorylation levels were similarly increased on insulin injection (about 1.5-fold) in *Chop*$^{-/-}$ and WT mice, and as total IRS1 and IRS2 levels were unaffected in *Chop*$^{-/-}$ mice compared with WT mice. The level of serine phosphorylation of IRS1 and IRS2, a negative regulator

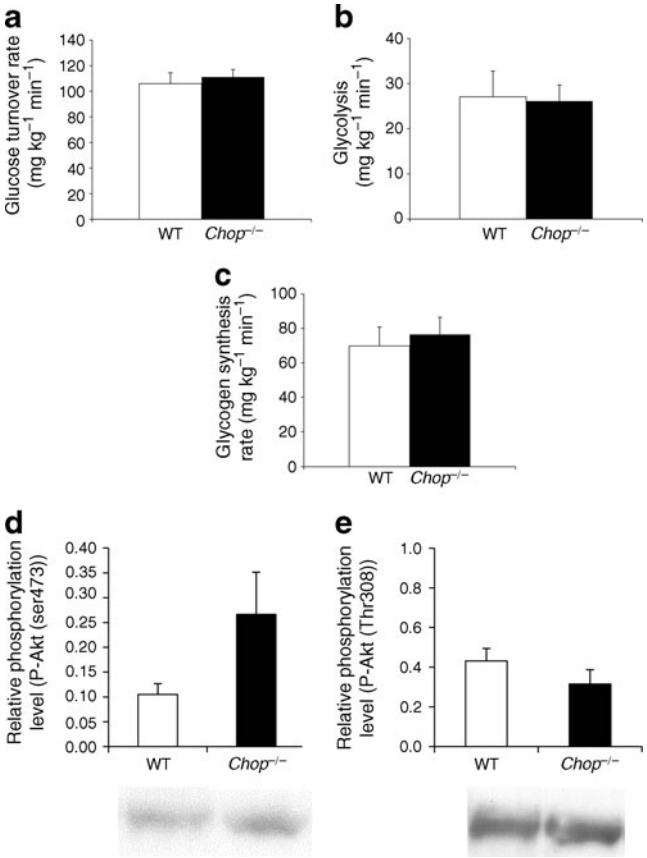

Fig. 5 Glucose turnover rate, glycolysis and glycogen synthesis during euglycaemic–hyperinsulinaemic clamps and p(Ser)AKT and p(Thr)AKT protein levels in *Chop*$^{-/-}$ and WT mice. Glucose turnover rate (**a**), glycolysis (**b**) and glycogen synthesis rate (**c**) during euglycaemic–hyperinsulinaemic clamps of female WT (white bars) and *Chop*$^{-/-}$ (black bars) mice at 24 weeks of age. Data are the means±SEM (n=6–8). **d,e** Protein phosphorylation levels of p(Ser)AKT (**d**) and p(Thr)AKT (**e**), measured in total liver extract of non-fasted female WT (white bars) and *Chop*$^{-/-}$ (black bars) mice at 24 weeks of age. Data are shown as means±SEM (n=4). A representative image of both WT and *Chop*$^{-/-}$ mice is shown

of insulin signalling, was similar in *Chop*$^{-/-}$ and WT mice. In addition, *Chop*$^{-/-}$ mice showed a trend (p=0.1) for increased protein level of suppressor of cytokine signalling 3 (SOCS3) compared with WT mice, whereas no changes in SOCS3 level could be observed on insulin stimulation (Fig. 6a–g).

Finally, insulin sensitivity was sustained in the skeletal muscles of *Chop*$^{-/-}$ mice, as the level of AKT serine phosphorylation was elevated to the same extent in the hind limbs of *Chop*$^{-/-}$ and WT mice on insulin stimulation (Fig. 6h).

Reduced inflammation in Chop$^{-/-}$ *mice* Immunohistochemical analysis of livers from 24-week-old *Chop*$^{-/-}$ and WT mice revealed a decreased presence of macrophages (7.9%±0.9 vs 15.6%±0.6 F4/80^{+}-stained macrophages per microscopic field in *Chop*$^{-/-}$ vs WT mice, respectively; p<0.001; Fig. 7a) and T lymphocytes (3.9%±0.2 vs 10.3%±0.6 CD3^{+}-stained T lymphocytes per microscopic field in *Chop*$^{-/-}$ vs WT mice, respectively; p<0.001; Fig. 7b) in *Chop*$^{-/-}$ mice compared with WT. The lower inflammatory status of liver was confirmed at the mRNA level, with lower expression of mRNA encoding the chemokines macrophage-derived chemokine (MDC) and interferon-inducible protein 10 (IP10) in the livers of 8-week-old *Chop*$^{-/-}$ mice (Fig. 7c). These differences persisted at 24 weeks when, in addition, lower levels of mRNA encoding the chemokines monocyte chemotactic protein 1 (MCP1) and the pro-inflammatory cytokine TNFα were detected in *Chop*$^{-/-}$ mice compared with WT (p<0.05; Fig. 7d).

In adipose tissue, a lower number of T lymphocytes (CD3^{+}) were observed in 24-week-old *Chop*$^{-/-}$ mice ($6.05\times10^{-5}\pm1.2\times10^{-5}$ vs $2.0\times10^{-4}\pm2.6\times10^{-5}$ CD3^{+} cells per μm^2 in *Chop*$^{-/-}$ vs WT mice, respectively; p<0.001), but there was no difference in macrophage (F4/80^{+}) infiltration (ESM Fig. 8a) or cytokine/chemokine mRNA expression

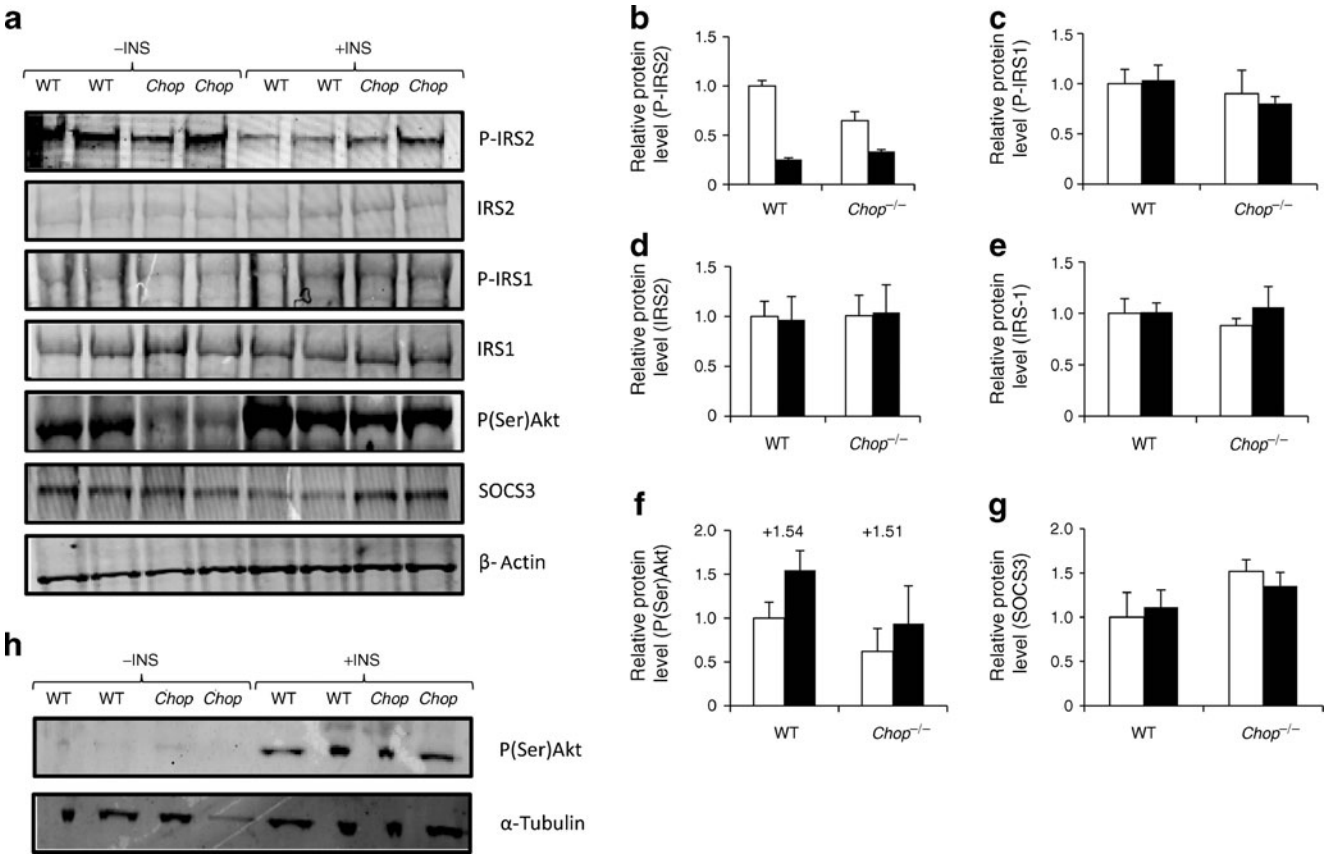

Fig. 6 Protein levels of different markers of insulin sensitivity in liver and skeletal muscle. **a** Western blotting for the indicated markers of insulin sensitivity and stable housekeeping protein β-actin on total liver extracts of female WT and *Chop*$^{-/-}$ mice, injected with either NaCl solution or 5 U insulin in the vena cava inferior, after an overnight fast at 24 weeks of age (n=4). A representative image of two mice/experimental group is shown. **b-g** Relative protein level normalised to the stable housekeeping protein β-actin in total liver extracts of female WT and *Chop*$^{-/-}$ mice, injected with either NaCl solution (white bars) or 5 U insulin (black bars) in the vena cava inferior, at 24 weeks of age. Results are means±SEM (n=4 independent experiments). **h** Western blotting for p(Ser)AKT and stable housekeeping protein α-tubulin on total hind-limb muscle extracts of female WT and *Chop*$^{-/-}$ mice, injected with either NaCl solution or 5 U insulin in the vena cava inferior at 24 weeks of age (n=4). A representative image of two mice/experimental group is shown. In **a** and **h**, *Chop* = *Chop*$^{-/-}$

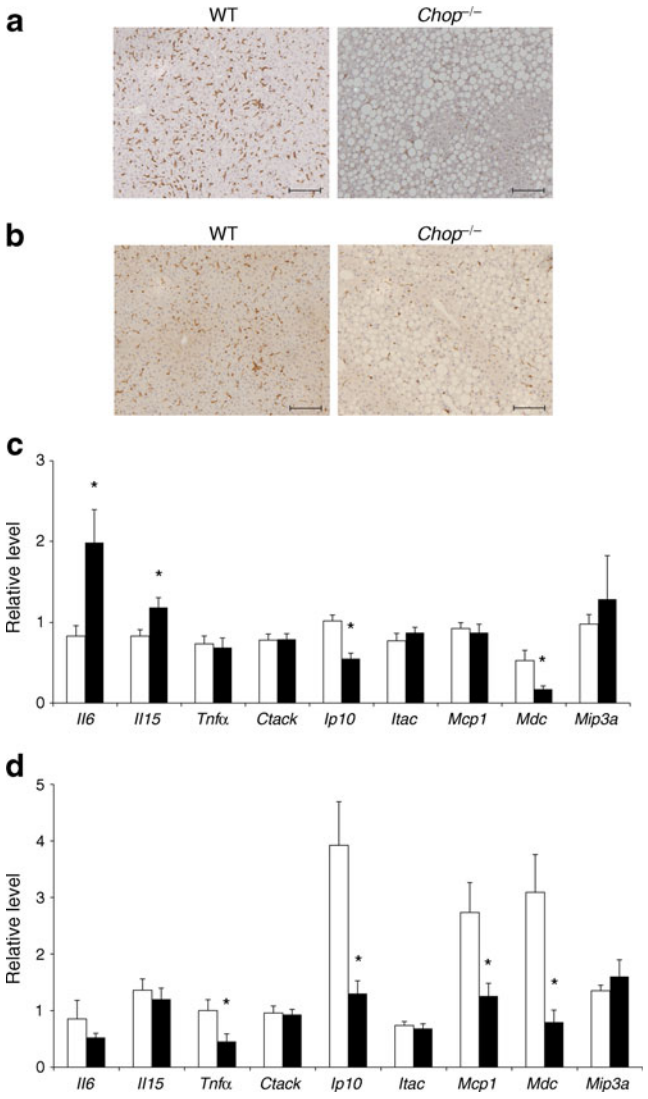

Fig. 7 Macrophage and lymphocyte infiltration and cytokine/chemokine mRNA expression in liver of WT and *Chop*$^{-/-}$ mice. Anti-F4/80 (**a**) and anti-CD3 (**b**) staining of representative liver sections of WT and *Chop*$^{-/-}$ mice at 24 weeks of age. Representative photomicrographs (×20 magnification) in two mice were captured with a Zeiss Axiovert microscope and analysed with the Axiovison Rel. 4.6 software. Levels of mRNA expression, normalised to the stable housekeeping gene *Rpl27*, of the indicated cytokines and chemokines in liver of female WT (white bars) and *Chop*$^{-/-}$ (black bars) mice at of 8 (**c**) and 24 (**d**) weeks of age. Data are shown as means±SEM (n=8). $^{*}p<0.05$ vs WT mice. (*Ctack* is also known as *Ccl27a; Itac* is also known as *Cxcl11*; *Mcp1* is also known as *Ccl2*; *Mdc* is also known as *Ccl22*; *Mip3a* is also known as *Ccl20*)

(ESM Fig. 8b). In addition, *Chop*$^{-/-}$ mice were characterised by lower plasma adiponectin levels compared with WT mice $p<0.01$; ESM Fig. 8c).

Peritoneal macrophages from *Chop*$^{-/-}$ mice showed lower expression levels of the pro-inflammatory cytokines *Il1*, *Il6* and *Tnfα* (also known as *Tnf*), the chemokine *Ip10* (also known as *Cxcl10*), *iNos* (also known as *Nos2*) and caspase-1 when stimulated in vitro with LPS (Fig. 8).

Discussion

Deletion of *Chop* disclosed an interesting phenotypic trait, presenting as increased body weight and fat mass, liver steatosis and absence of insulin resistance. The observed weight gain and increased body mass in female *Chop*$^{-/-}$ mice are in line with previous results [9, 23]. *Chop*$^{-/-}$ mice had a similar energy expenditure, but showed a trend for increased food uptake. This observation is in contrast with a previous report [9]. However, it should be stated that our measurement of food intake is more reliable, as it was determined using extremely sensitive metabolism cages, whereas Ariyama *et al.* did not use this gold standard. The lower RQ of *Chop*$^{-/-}$ compared with WT mice, demonstrating a higher lipid over carbohydrate oxidation, indicates qualitative changes in energy expenditure. It is unlikely that *Chop* deletion induces obesity by adipogenesis as similar expression levels of *C/ebpα* and *Pparγ* and a decreased expression level of *C/ebpβ* were observed in the abdominal fat of *Chop*$^{-/-}$ mice. These results are in contrast with previous findings showing increased protein levels of C/EBPβ and of the 30 kDa truncated form of C/EBPα in perimetrial fat tissue of female *Chop*$^{-/-}$ mice, whereas expression of the 42 kDa form of C/EBPα was reduced [9]. Whereas we measured mRNA levels, Ariyama *et al.* determined protein levels of the C/EBPs. As discussed below, mRNA and protein levels do not always correlate. As both forms of C/EBPα are produced by alternative initiation of translation and as one isoform was found to be increased whereas the other was found to be decreased, it is plausible that total *C/ebpα* mRNA levels, as measured in our study, are unchanged. Furthermore, we cannot rule out differences in levels between abdominal fat tissue (our study) and perimetrial fat tissue [9]. Finally, Ariyama *et al.* performed their estimations of C/EBP level at 12 months of age, whereas we performed them at 24 weeks of age. In general, it should be stated that in the paper by Ariyama *et al.*, little information is given about the age of the mice at time of the analyses and the diet used. *Chop*$^{-/-}$ mice were also characterised by increased BMC and BMD, even at 4 weeks of age, suggesting a regulatory role for CHOP in bone development.

Altered thermogenesis and physical activity do not play a predominant role in the obese phenotype of *Chop*$^{-/-}$ mice. The decreased serum oestrogen levels previously found [9] could contribute to increased fat mass, but as a similar decrease in oestrogen levels without any effect on abdominal fat mass was observed in male *Chop*$^{-/-}$ mice in the same study, differences in oestrogen levels probably cannot explain the abdominal obesity. Thus, to date, the cause of the observed obesity remains unclear, as of the processes that were tested only nutrient consumption showed a trend to be abnormal.

As targeted disruption of *Chop* delays the onset of diabetes in heterozygous Akita mice [8], we hypothesised that deletion

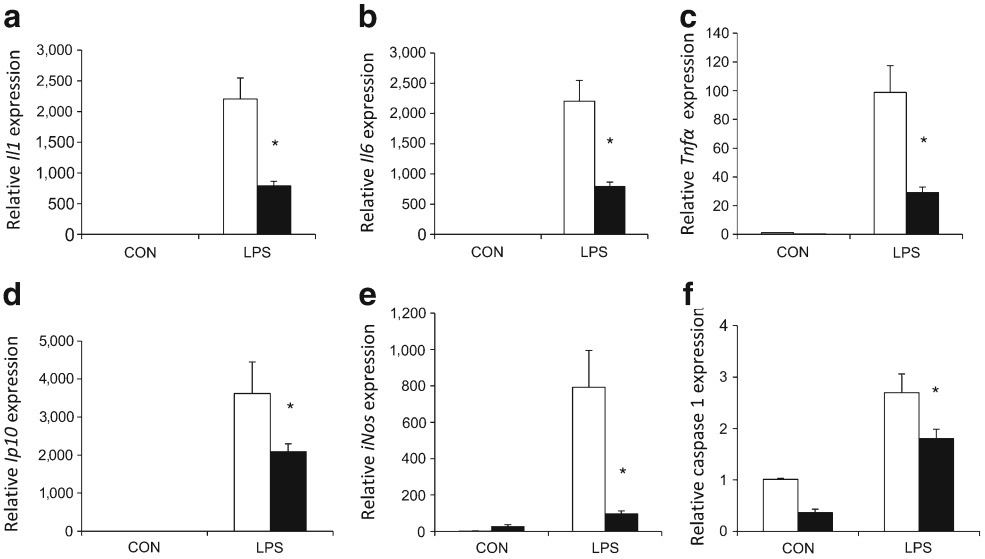

Fig. 8 Cytokine and chemokine mRNA expression in intraperitoneal macrophages of female WT and *Chop*$^{-/-}$ mice. Levels of mRNA expression, normalised to the stable housekeeping gene *Rpl27*, of *Il1* (**a**), *Il6* (**b**), *Tnfα* (**c**), *Ip10* (**d**), *iNos* (**e**) and caspase-1 (**f**) in isolated intraperitoneal macrophages of 8-week-old female WT (white bars) and *Chop*$^{-/-}$ (black bars) mice, stimulated with LPS or not (control) for 6 h. Data are shown as means±SEM (n=8). $^{*}p<0.05$ vs WT mice. Con, control

of *Chop* could protect beta cells from apoptosis and delay the onset of type 2 diabetes. This hypothesis was strengthened by recent observations that knockdown of *Chop* by small interfering RNA protects adult beta cells against NEFA and chemical ER stressors [24]. We observed increased islet size in *Chop*$^{-/-}$ mice, confirming previous observations [23], but *Chop*$^{-/-}$ islets were not protected against beta cell death induced by NEFA or thapsigargin in vitro. These observations are in line with previous observations that islets isolated from WT and *Chop*$^{-/-}$ mice did not reveal any differences in acute toxicity after streptozotocin treatment [23]. As *Chop*$^{-/-}$ mice showed milder glucose intolerance under high-fat-diet conditions and after streptozotocin administration, they suggested that *Chop* deletion rather preserves beta cell function and influences cell recovery and/or function [23].

Electron microscopy of beta cells did not reveal differences between *Chop*$^{-/-}$ and WT mice. This absence of a clear effect on beta cells may be due to the multiple effects of CHOP in vivo and to putative adaptation to long-term lack of CHOP in beta cells, starting in embryonic life.

The increase in protein levels of ER-stress markers in *Chop*$^{-/-}$ mice is in line with previous reports, demonstrating that excessive fat deposition leads to hypertrophy of adipocytes, activating an ER stress response [25]. Of note, there is a discrepancy between mRNA and protein levels. In this view, we have previously shown that changes in mRNA levels initiating the unfolded protein response are not translated into protein changes. Moreover, we stated an important role for post-translational modifications in the regulation of ER stress [26, 27]. Activation of ER stress induces an increased release of NEFA, adipokines and inflammatory mediators [28, 29], triggering infiltration and activation of macrophages in adipose tissue, contributing to insulin resistance [30, 31]. These infiltrating immune cells further stimulate secretion of adipokines from adipocytes [31] and secrete pro-inflammatory cytokines of which TNFα and IL-6 are implicated in the induction of insulin resistance [32, 33]. The absence of inflammation around the hypertrophic adipocytes of *Chop*$^{-/-}$ mice contrasts with the increased numbers of resident macrophages in adipose tissue of obese individuals [34] and suggests that CHOP provides a crucial pro-inflammatory signal in fat. In contrast to a previous finding [9], adiponectin levels were lower in plasma of *Chop*$^{-/-}$ compared with WT mice. This controversy could be explained by differences in, for example, age or diet used, which are not stated in the previous report. It could be speculated that CHOP is an important link between the activated ER-stress response and the induction of inflammation in adipocytes, an effect independent of adiponectin. It has been demonstrated extensively that the presence of ectopic fat in insulin sensitive tissues contributes to insulin resistance [35, 36]. *Chop*$^{-/-}$ mice are characterised by massive liver steatosis, but remain perfectly insulin sensitive and glucose tolerant and have normal circulating NEFA and triacylglycerol levels.

The expression level of major regulatory enzymes of lipogenesis was unchanged in *Chop*$^{-/-}$ mice, both at the mRNA and protein level, ruling out increased production of triacylglycerol in the liver. A reduction in VLDL secretion by the liver of *Chop*$^{-/-}$ mice could be a possible explanation for the observed steatosis, as blocking VLDL secretion causes hepatic steatosis without affecting hepatic glucose production, hepatic insulin signalling, peripheral lipid stores or insulin sensitivity in mice [37]. Despite massive steatosis, no signs of steatohepatitis were present. On the contrary, there was less infiltration of macrophages and T lymphocytes and lower transaminase levels. Others have previously suggested that chronic steatosis-associated inflammation leads to insulin resistance [38]. The lower levels of immune cells in liver were paralleled by lower mRNA expression of chemokines, already noticeable in 8-week-old *Chop*$^{-/-}$ mice. Some chemokines,

such as MCP1, are induced in the adipose tissue of obese mice and may contribute to the development of insulin resistance and de-differentiation of adipocytes [39–41]. Blocking the MCP1 receptor ameliorates insulin resistance and steatosis in *db*/*db* mice [42], so decreased hepatic *Mcp1* expression in *Chop*$^{-/-}$ mice could contribute to decreased macrophage recruitment and amelioration of insulin sensitivity. Additionally, inflammation in *Chop*$^{-/-}$ mice could also be suppressed by SOCS3, as increases in SOCS3 protein levels, although minor, were observed in liver. It has been demonstrated that SOCS3 suppresses cytokine-mediated signal transduction and liver apoptosis induced by several pathogen-derived agonists, leading to increased survival rates [43]. Nevertheless, other reports demonstrated that hepatic SOCS3 is a negative regulator of insulin sensitivity by interfering with correct IRS1 and IRS2 phosphorylation, inhibiting downstream insulin signalling. Deletion of hepatic *Socs3* increases liver insulin sensitivity in mice fed a control diet, but promotes development of obesity and systemic insulin resistance by mimicking chronic inflammation [44, 45]. However, insulin signalling was sustained in the livers of *Chop*$^{-/-}$ mice on insulin stimulation, indicating that in our model, SOCS3 has a role in maintaining insulin sensitivity by suppressing inflammation.

As steatosis is associated with ER stress [46] and as activation of ER stress is related to the induction of inflammatory pathways, absence of ER stress in *Chop*$^{-/-}$ mice, both at the mRNA and protein level, may also contribute to the absence of inflammation in liver and to the maintenance of insulin sensitivity.

Finally, *Chop*$^{-/-}$ mice have no ectopic fat deposition in muscle and a preserved AKT serine phosphorylation on insulin stimulation, which could contribute to preserving peripheral insulin sensitivity in these mice [47].

Recent evidence points to a role of CHOP in various inflammatory diseases, such as LPS-induced lung damage [10, 11], chemically induced pancreatitis [13] and experimental colitis [12]. Here, we demonstrate that CHOP is indeed central in the inflammatory response of liver, fat and macrophages, as peritoneal macrophages from *Chop*$^{-/-}$ mice exhibit a blunted inflammatory response to LPS. The exact downstream targets of CHOP involved in inflammation are not well understood, but CHOP could induce inflammation via several pathways. As such, CHOP induces activation of ERO1α, leading to exaggerated production of ROS [4–6, 48], which promotes the production of pro-inflammatory cytokines [49]. In addition, CHOP directly regulates the IL-8 promoter [50] and can induce IL-1β production through activation of caspase-11 [11].

Based on the present observations we suggest that *Chop*$^{-/-}$ mice remain insulin sensitive in spite of severe obesity and ectopic fat deposition because *Chop* deletion prevents the inflammatory reaction. This indicates that it is not the fat mass per se, but rather the associated inflammatory status that determines the onset of insulin resistance. We propose that CHOP is a crucial mediator in the induction of insulin resistance, serving as a link between fat accumulation and insulin resistance.

Acknowledgements The technical experience of J. Laureys and J. Depovere is greatly appreciated. We thank S. Akira (Osaka University, Japan) and M. Mori (Kumamoto University, Japan) for their kind gift of *Chop*$^{-/-}$ mice. We also thank D. Vanderschueren (Catholic University Leuven, Belgium) for the use of the PIXImus densitometer and J. Buyse (Catholic University Leuven, Belgium) for the plasma T3 and T4 measurements. Electron microscopy was carried out by P. Baatsen at the Electron Microscopy Facility of the VIB department for Molecular and Developmental Genetics, KULeuven. Metabolic studies were performed by the Phenotyping Service Platform Anexplo (Genotoul, IFR BM-T), Toulouse.

Funding This work was supported by the European Union (STREP SaveBeta no. 036,903 in the Framework Program 6), the Catholic University of Leuven (2009/10), the Flemish Research Foundation (FWO G.0552.06 and G.0649.08), the Belgium Program on Interuniversity Poles of Attraction initiated by the Belgian State (P6/40), the Juvenile Diabetes Research Foundation International (1-2008-536) and an unrestricted educational grant from Merck Sharp & Dohme. C. Gysemans is supported by a postdoctoral fellowship (FWO), A. K. Cardozo is a research associate of the Fonds National de la Recherche Scientifique (FNRS). M. Cnop is supported by the FNRS Médicale (FRSM) and C. Mathieu by a clinical research fellowship (FWO).

Duality of interest The authors declare that there is no duality of interest associated with this manuscript.

Contribution statement MM, LO, CG, AW, AKC, EV, JPMC, TG, MC, DLE, RB and CM contributed to the conception and design, analysis and interpretation of data, drafting or revising of the article and gave their final approval of the article to be published.

References

1. Ozcan L, Ergin AS, Lu A et al (2009) Endoplasmic reticulum stress plays a central role in development of leptin resistance. Cell Metab 9:35–51
2. Ozcan U, Cao Q, Yilmaz E et al (2004) Endoplasmic reticulum stress links obesity, insulin action, and type 2 diabetes. Science 306:457–461
3. Zhang X, Zhang G, Zhang H, Karin M, Bai H, Cai D (2008) Hypothalamic IKKbeta/NF-kappaB and ER stress link overnutrition to energy imbalance and obesity. Cell 135:61–73
4. Marciniak SJ, Yun CY, Oyadomari S et al (2004) CHOP induces death by promoting protein synthesis and oxidation in the stressed endoplasmic reticulum. Genes Dev 18:3066–3077
5. Wang XZ, Kuroda M, Sok J et al (1998) Identification of novel stress-induced genes downstream of chop. EMBO J 17:3619–3630
6. Gotoh T, Terada K, Oyadomari S, Mori M (2004) hsp70-DnaJ chaperone pair prevents nitric oxide- and CHOP-induced apoptosis by inhibiting translocation of Bax to mitochondria. Cell Death Differ 11:390–402

7. Kayo T, Koizumi A (1998) Mapping of murine diabetogenic gene mody on chromosome 7 at D7Mit258 and its involvement in pancreatic islet and beta cell development during the perinatal period. J Clin Invest 101:2112–2118
8. Oyadomari S, Koizumi A, Takeda K et al (2002) Targeted disruption of the Chop gene delays endoplasmic reticulum stress-mediated diabetes. J Clin Invest 109:525–532
9. Ariyama Y, Shimizu H, Satoh T et al (2007) Chop-deficient mice showed increased adiposity but no glucose intolerance. Obesity (Silver Spring) 15:1647–1656
10. Endo M, Oyadomari S, Suga M, Mori M, Gotoh T (2005) The ER stress pathway involving CHOP is activated in the lungs of LPS-treated mice. J Biochem 138:501–507
11. Endo M, Mori M, Akira S, Gotoh T (2006) C/EBP homologous protein (CHOP) is crucial for the induction of caspase-11 and the pathogenesis of lipopolysaccharide-induced inflammation. J Immunol 176:6245–6253
12. Namba T, Tanaka K, Ito Y et al (2009) Positive role of CCAAT/enhancer-binding protein homologous protein, a transcription factor involved in the endoplasmic reticulum stress response in the development of colitis. Am J Pathol 174:1786–1798
13. Suyama K, Ohmuraya M, Hirota M et al (2008) C/EBP homologous protein is crucial for the acceleration of experimental pancreatitis. Biochem Biophys Res Commun 367:176–182
14. Woo CW, Cui D, Arellano J et al (2009) Adaptive suppression of the ATF4-CHOP branch of the unfolded protein response by toll-like receptor signalling. Nat Cell Biol 11:1473–1480
15. Mahadevan NR, Rodvold J, Sepulveda H, Rossi S, Drew AF, Zanetti M (2011) Transmission of endoplasmic reticulum stress and pro-inflammation from tumor cells to myeloid cells. Proc Natl Acad Sci U S A 108:6561–6566
16. Pereira RC, Stadmeyer LE, Smith DL, Rydziel S, Canalis E (2007) CCAAT/Enhancer-binding protein homologous protein (CHOP) decreases bone formation and causes osteopenia. Bone 40: 619–626
17. Oyadomari S, Takeda K, Takiguchi M et al (2001) Nitric oxide-induced apoptosis in pancreatic beta cells is mediated by the endoplasmic reticulum stress pathway. Proc Natl Acad Sci U S A 98:10845–10850
18. Van Veldhoven PP, Swinnen JV, Esquenet M, Verhoeven G (1997) Lipase-based quantitation of triacylglycerols in cellular lipid extracts: requirement for presence of detergent and prior separation by thin-layer chromatography. Lipids 32:1297–1300
19. Mizuno K, Toyosato M, Yabumoto S, Tanimizu I, Hirakawa H (1980) A new enzymatic method for colorimetric determination of free fatty acids. Anal Biochem 108:6–10
20. Darras VM, Visser TJ, Berghman LR, Kuhn ER (1992) Ontogeny of type I and type III deiodinase activities in embryonic and posthatch chicks: relationship with changes in plasma triiodothyronine and growth hormone levels. Comp Biochem Physiol Comp Physiol 103:131–136
21. Burcelin R, Crivelli V, Dacosta A, Roy-Tirelli A, Thorens B (2002) Heterogeneous metabolic adaptation of C57BL/6 J mice to high-fat diet. Am J Physiol Endocrinol Metab 282:E834–E842
22. Bard-Chapeau EA, Hevener AL, Long S, Zhang EE, Olefsky JM, Feng GS (2005) Deletion of Gab1 in the liver leads to enhanced glucose tolerance and improved hepatic insulin action. Nat Med 11:567–571
23. Song B, Scheuner D, Ron D, Pennathur S, Kaufman RJ (2008) Chop deletion reduces oxidative stress, improves beta cell function, and promotes cell survival in multiple mouse models of diabetes. J Clin Invest 118:3378–3389
24. Cunha DA, Hekerman P, Ladriere L et al (2008) Initiation and execution of lipotoxic ER stress in pancreatic beta-cells. J Cell Sci 121:2308–2318
25. Hummasti S, Hotamisligil GS (2010) Endoplasmic reticulum stress and inflammation in obesity and diabetes. Circ Res 107: 579–591
26. Maris M, Waelkens E, Cnop M et al (2011) Oleate-induced beta cell dysfunction and apoptosis: a proteomic approach to glucolipotoxicity by an unsaturated fatty acid. J Proteome Res 10:3372–3385
27. Maris M, Ferreira GB, D'Hertog W et al (2010) High glucose induces dysfunction in insulin secretory cells by different pathways: a proteomic approach. J Proteome Res 9:6274–6287
28. Bastard JP, Maachi M, Lagathu C et al (2006) Recent advances in the relationship between obesity, inflammation, and insulin resistance. Eur Cytokine Netw 17:4–12
29. Boden G, Duan X, Homko C et al (2008) Increase in endoplasmic reticulum stress-related proteins and genes in adipose tissue of obese, insulin-resistant individuals. Diabetes 57:2438–2444
30. Xu H, Barnes GT, Yang Q et al (2003) Chronic inflammation in fat plays a crucial role in the development of obesity-related insulin resistance. J Clin Invest 112:1821–1830
31. Bouloumie A, Curat CA, Sengenes C, Lolmede K, Miranville A, Busse R (2005) Role of macrophage tissue infiltration in metabolic diseases. Curr Opin Clin Nutr Metab Care 8:347–354
32. Rotter V, Nagaev I, Smith U (2003) Interleukin-6 (IL-6) induces insulin resistance in 3T3-L1 adipocytes and is, like IL-8 and tumor necrosis factor-alpha, overexpressed in human fat cells from insulin-resistant subjects. J Biol Chem 278:45777–45784
33. Hotamisligil GS, Peraldi P, Budavari A, Ellis R, White MF, Spiegelman BM (1996) IRS-1-mediated inhibition of insulin receptor tyrosine kinase activity in TNF-alpha- and obesity-induced insulin resistance. Science 271:665–668
34. Wellen KE, Hotamisligil GS (2005) Inflammation, stress, and diabetes. J Clin Invest 115:1111–1119
35. Szendroedi J, Roden M (2009) Ectopic lipids and organ function. Curr Opin Lipidol 20:50–56
36. Lettner A, Roden M (2008) Ectopic fat and insulin resistance. Curr Diab Rep 8:185–191
37. Minehira K, Young SG, Villanueva CJ et al (2008) Blocking VLDL secretion causes hepatic steatosis but does not affect peripheral lipid stores or insulin sensitivity in mice. J Lipid Res 49:2038–2044
38. Ogawa W, Kasuga M (2008) Cell signaling. Fat stress and liver resistance. Science 322:1483–1484
39. Kanda H, Tateya S, Tamori Y et al (2006) MCP-1 contributes to macrophage infiltration into adipose tissue, insulin resistance, and hepatic steatosis in obesity. J Clin Invest 116:1494–1505
40. Weisberg SP, Hunter D, Huber R et al (2006) CCR2 modulates inflammatory and metabolic effects of high-fat feeding. J Clin Invest 116:115–124
41. Sartipy P, Loskutoff DJ (2003) Monocyte chemoattractant protein 1 in obesity and insulin resistance. Proc Natl Acad Sci U S A 100:7265–7270
42. Tamura Y, Sugimoto M, Murayama T et al (2008) Inhibition of CCR2 ameliorates insulin resistance and hepatic steatosis in db/db mice. Arterioscler Thromb Vasc Biol 28:2195–2201
43. Jo D, Liu D, Yao S, Collins RD, Hawiger J (2005) Intracellular protein therapy with SOCS3 inhibits inflammation and apoptosis. Nat Med 11:892–898
44. Torisu T, Sato N, Yoshiga D et al (2007) The dual function of hepatic SOCS3 in insulin resistance in vivo. Genes Cells 12:143–154
45. Ueki K, Kondo T, Kahn CR (2004) Suppressor of cytokine signaling 1 (SOCS-1) and SOCS-3 cause insulin resistance through inhibition of tyrosine phosphorylation of insulin receptor substrate proteins by discrete mechanisms. Mol Cell Biol 24:5434–5446

46. Fu S, Yang L, Li P et al (2011) Aberrant lipid metabolism disrupts calcium homeostasis causing liver endoplasmic reticulum stress in obesity. Nature 473:528–531
47. Bruss MD, Arias EB, Lienhard GE, Cartee GD (2005) Increased phosphorylation of Akt substrate of 160 kDa (AS160) in rat skeletal muscle in response to insulin or contractile activity. Diabetes 54:41–50
48. Oyadomari S, Mori M (2004) Roles of CHOP/GADD153 in endoplasmic reticulum stress. Cell Death Differ 11:381–389
49. Bulua AC, Simon A, Maddipati R et al (2011) Mitochondrial reactive oxygen species promote production of proinflammatory cytokines and are elevated in TNFR1-associated periodic syndrome (TRAPS). J Exp Med 208:519–533
50. Vij N, Amoako MO, Mazur S, Zeitlin PL (2008) CHOP transcription factor mediates IL-8 signaling in cystic fibrosis bronchial epithelial cells. Am J Respir Cell Mol Biol 38:176–184